Radboud Repository

Radboud University Nijmegen

PDF hosted at the Radboud Repository of the Radboud University Nijmegen

The following full text is a publisher's version.

For additional information about this publication click this link.
http://hdl.handle.net/2066/26157

Please be advised that this information was generated on 2017-12-05 and may be subject to change.

JOURNAL OF VIROLOGY, Jan. 1997, p. 686–696
0022-538X/97/$04.00+0
Copyright © 1997, American Society for Microbiology
Vol. 71, No. 1

Kissing of the Two Predominant Hairpin Loops in the Coxsackie B Virus 3′ Untranslated Region Is the Essential Structural Feature of the Origin of Replication Required for Negative-Strand RNA Synthesis

WILLEM J. G. MELCHERS,[1]* JOOST G. J. HOENDEROP,[1] HILBERT J. BRUINS SLOT,[2] CORNELIS W. A. PLEIJ,[3] EVGENY V. PILIPENKO,[4] VADIM I. AGOL,[4] AND JOEP M. D. GALAMA[1]

Department of Medical Microbiology, University of Nijmegen, 6500 HB Nijmegen,[1] CAOS/CAMM Center, University of Nijmegen, 6500 GL Nijmegen,[2] and Leiden Institute of Chemistry, University of Leiden, 2300 RA Leiden,[3] The Netherlands, and Institute of Poliomyelitis and Viral Encephalitides, Russian Academy of Medical Sciences, Moscow Region 142782, Russia[4]

Received 30 January 1996/Accepted 1 October 1996

Higher-order RNA structures in the 3′ untranslated region (3′UTR) of enteroviruses are thought to play a pivotal role in viral negative-strand RNA synthesis. The structure of the 3′UTR was predicted by thermodynamic calculations using the STAR (structural analysis of RNA) computer program and experimentally verified using chemical and enzymatic probing of in vitro-synthesized RNA. A possible pseudoknot interaction between the 3D polymerase coding sequence and domain Y and a "kissing" interaction between domains X and Y was further studied by mutational analysis, using an infectious coxsackie B3 virus cDNA clone (domain designation as proposed by E. V. Pilipenko, S. V. Maslova, A. N. Sinyakov, and V. I. Agol (Nucleic Acids Res. 20:1739–1745, 1992). The higher-order RNA structure of the 3′UTR appeared to be maintained by an intramolecular kissing interaction between the loops of the two predominant hairpin structures (X and Y) within the 3′UTR. Disturbing this interaction had no effect on viral translation and processing of the polyprotein but exerted a primary effect on viral replication, as was demonstrated in a subgenomic coxsackie B3 viral replicon, in which the capsid P1 region was replaced by the luciferase gene. Mutational analysis did not support the existence of the pseudoknot interaction between hairpin loop Y and the 3D polymerase coding sequence. Based on these experiments, we constructed a three-dimensional model of the 3′UTR of coxsackie B virus that shows the kissing interaction as the essential structural feature of the origin of replication required for its functional competence.

Coxsackie B viruses are small RNA viruses with a genome of approximately 7,500 bases (47). Replication is initiated in the cytoplasm of the host cell by the synthesis of a complementary RNA strand of negative polarity (41). This double-stranded RNA intermediary is subsequently encapsidated by vesicles derived from the rough endoplasmatic reticulum (7) to produce the replication complex, a membranous double-stranded RNA complex containing virally encoded proteins and cellular factors (6). The 5′ untranslated region (5′UTR) contains regions with functional domains for positive-strand RNA synthesis (2, 35). Andino et al. (3) have recently described the existence of a ribonucleoprotein complex formed at the 5′ end of poliovirus RNA which contained a cloverleaf-like structure formed by the first part of the 5′UTR interacting with the virus 3CD precursor and a cellular factor. They proposed a *trans*-initiation model for the synthesis of positive-strand RNA in which the synthesis of a newly formed positive-strand RNA molecule allows a new cloverleaf-like structure to form, with the subsequent formation of a new ribonucleoprotein complex which can then catalyze the initiation of the next positive-strand RNA (3). The $3D^{pol}$ catalyzes both positive-strand as well as negative-strand RNA synthesis, and it is thought that VPg is uridylated for negative-strand RNA synthesis to form an uridylated VPg-dUU which subsequently acts as a primer for the initiation of negative-strand RNA synthesis (44).

Higher-order RNA structures in the 3′UTR are thought to play a role in the initiation of negative-strand RNA synthesis. Several attempts have been made to elucidate the structure of the enterovirus 3′UTR (13, 27). The secondary structures predicted for the enterovirus 3′UTR all seem to point to a conformation consisting of two (X and Y) to three (X, Y, and Z) hairpin structures, in which the poly(A) tract is partly included (13, 27). Although the functional aspects of these secondary structures have not yet been elucidated, it has been suggested that interactions occur either between the two predominant loops (X and Y) within the 3′UTR (27) or between one hairpin loop (Y) and the flanking coding sequences of the 3D RNA polymerase (13), forming two higher-order tertiary RNA structures. However, the actual existence of either one of these higher-order RNA structures has yet to be proven.

To gain insight into the mechanisms involved in virus negative-strand RNA synthesis, we have further characterized the enterovirus 3′UTR by predicting its secondary and tertiary structures using thermodynamics-based structure calculations, verifying it by chemical and enzymatic probing, and introducing site-directed mutations in an infectious coxsackie B3 virus cDNA clone. The effect of these mutations on virus viability and growth characteristics, RNA synthesis, and viral protein synthesis and processing were determined, and based on the

* Corresponding author. Mailing address: Dept. of Medical Microbiology, University of Nijmegen, P.O. Box 9101, 6500 HB Nijmegen, The Netherlands. Phone: 31-24-3617574. Fax: 31-24-3540216. E-mail: W.Melchers@mmb.azn.nl.

TABLE 1. Mutagenesis oligonucleotides

Mutation	Oligonucleotide sequence
pCB3-3′UTR:ACCG$_{7349-7352}$→UGGC	5-TACCGTTATCTGGTTGCCATAGCACAGTAGGGTT-3
pCB3-3′UTR:CGGU$_{7392-7395}$→GCCA	5-AAAAAAAAAAACCGCTGGCAATGCGGAGAATTTA-3
pCB3-3D:UGGU$_{7282-7285}$→GCCA	5-TCTAAAAGGAGTCCATGGTCTTCCTGCGTAGAGT-3
pCB3-3′UTR:GUGC$_{7343-7346}$→CAGG/ GUAC$_{7365-7368}$→CUUG	5-GAATTTACCCCTACTCAAGCGTTATCTGGTTCGGTTACCTGAGTAGGGTTAAGCCA-3
pCB3-3D:UUG$_{7285-7287}$→CUU	5-AAAAGGAGTCAAGCCACTTCCTG-3
pCB3-3′UTR:C$_{7392}$→G	5-TTTCCGCACCCAATGCGGAGA-3
pCB3-3′UTR:G$_{7352}$→C	5-TTATCTGGTTGGGTTAGCACA-3
pCB3-3′UTR:C$_{7392}$→U	5-TTTCCGCACCAAATGCGGAGA-3
pCB3-3′UTR:G$_{7352}$→A	5-TTATCTGGTTTGGTTAGCACA-3
pCB3-3′UTR:U$_{7391}$→G	5-TTCCGCACCGCATGCGGAGAA-3
pCB3-3′UTR:A$_{7353}$→C	5-GTTATCTGGTGCGGTTAGCAC-3

structure, a three-dimensional model of the 3′UTR was developed.

MATERIALS AND METHODS

Prediction of the enterovirus 3′UTR structure. To calculate the secondary structure of the coxsackie B virus 3′UTR, we employed the STAR (structural analysis of RNA) computer algorithm (1). The STAR program simulates RNA folding by stepwise addition of stems to the structure formed at the preceding steps. The predicted structure starts with the stem-loop with the lowest free energy and then adds new stem-loops that are consistent with those already incorporated, according to their stability. These include base pair interactions of nucleotides in a loop with complementary nucleotides in single-stranded regions, as well as nucleotides in other loops. Stabilization caused by stacking of double helices is also taken into account. STAR is therefore able to predict not only secondary structures but also aspects of tertiary structures (1). Part of the 3D polymerase coding region was analyzed together with the complete 3′UTR and the poly(A) tract (nucleotides [nt] 7271 to 7410) to develop a model of the structure of the coxsackie B3 virus.

Oligonucleotide-directed site-specific mutagenesis. A full-length DNA copy of coxsackie B3 virus (pCB3/T7) which was cloned behind a T7 RNA polymerase promoter was used in the experiments (15). The *Xba*I (nt 4947) to *Xba*I (MCS pCB3/T7) fragment was subcloned into phagemid pALTER-1, and mutations were introduced using the Altered Sites in vitro mutagenesis system (Promega) according to the recommendations of the manufacturer. Synthetic oligonucleotides (Isogen BioScience, Maarsen, The Netherlands) were used to introduce site-specific mutations (Table 1).

The nucleotide sequences of the mutated cDNAs were verified by dideoxy chain termination sequence analysis of plasmid DNA with oligonucleotide 5′-G TTGTTTGACCCTCCCCGCG-3′ (complementary to nt 7241 to 7260) using the Ampli Cycle sequencing kit according to the instructions of the manufacturer (Perkin-Elmer). The mutated fragment was cloned in pCB3/T7-*Xba*I for further characterization.

Chemical and enzymatic probing of coxsackie B3 virus 3′UTR. Chemical and enzymatic probing was performed on wild-type pCB3/T7 copy RNA and on the mutated-copy RNAs (Table 1). Plasmids were linearized by digestion with *Sal*I. Copy RNA transcripts were generated and purified, using a protocol described previously (26). Full-length copy RNA transcripts (1 μg) were used for the chemical and enzymatic probing. The conditions used to treat the full-length copy RNA with dimethyl sulfate (DMS), RNase T_1, cobra venom nuclease V_1, and *Bacillus cereus* and *Phy M* nucleases have been described in detail previously (25–27), as have those for locating the modified nucleotides or cleavage sites by the primer extension technique. The cDNA products were electrophoretically separated on 10 and 20% polyacrylamide–8 M urea slab gels.

Cells and viruses. Virus propagations and RNA transfections were performed with Vero cells grown in minimal essential medium (MEM) supplemented with 10% fetal bovine serum (GIBCO). After infection, the cells were fed with MEM containing 3% fetal bovine serum. After transfection, MEM containing 10% fetal bovine serum was added to the cells (45). Virus yields were determined by endpoint titrations using eight replicates of serial 10-fold dilutions in 96-well plates containing Vero cell monolayers (37). The 50% tissue culture infective dose ($TCID_{50}$) was calculated according to the probit method of Reed and Muench (31).

Transcription and transfection of cells with copy RNA transcripts. Plasmids were linearized by digestion with *Sal*I, extracted with phenol-chloroform, and ethanol precipitated. Copy RNA transcripts obtained from two separate clones of each mutation were generated in a 100-μl reaction mixture containing 2 μg of linearized template DNA, 40 mM Tris HCl (pH 7.5), 10 mM NaCl, 6 mM $MgCl_2$, 2 mM spermidine, 2.5 mM each nucleoside triphosphate, 100 U of RNase inhibitor (Pharmacia), and 30 U of T7 RNA polymerase (Pharmacia), and 2 μl was analyzed on a 1% agarose gel. Copy RNA (4 μg) was used for transfection of Vero cells using the DEAE-dextran method as previously described (45). After transfection, the cells were washed three times with phosphate-buffered saline, overlaid with cell culture medium, and incubated in duplicate at 33 and 36°C. When virus growth was observed, the cells were incubated until the cytopathic effect (CPE) was complete. When no CPE was observed, the cells were incubated until the cytopathic effect (CPE) was complete. When no CPE was observed 5 days after transfection, the cell cultures were subjected to three cycles of freezing and thawing, and 250 μl was subsequently passaged to fresh Vero cell monolayers. When the CPE was complete, the cultures were subjected to three cycles of freezing and thawing and the viruses were stored in 1-ml aliquots at −80°C. When no CPE was observed 5 days after passage, the mutations were considered to be lethal.

Single-cycle growth curves. The kinetics of viral growth were estimated by measuring the virus yields in single-cycle infections. Vero cell monolayers (5×10^6 cells) grown in 25-cm^2 flasks were infected with wild-type and mutant viruses at a multiplicity of infection (MOI) of 1 $TCID_{50}$ per cell. After 30 min of adsorption at room temperature, the cells were washed three times with MEM, and 5 ml of cell culture medium was added. The cells were grown at 33, 36, and 39°C for 4, 6, and 8 h. Viruses were released by three successive cycles of freezing and thawing, and titers were determined as described above.

Sequence analysis of 3′UTR of mutant viruses. Total RNA was isolated from 100 μl of cellular lysates obtained from the 8-h time point of the growth curve, using a single extraction procedure with guanidinium thiocyanate-phenol-chloroform (9). Mutated RNA was PCR amplified, using a poly(T) primer and a primer located in the 3D coding region (5′-GTTGTTTGACCCTCCCCGCG-3′; nt 7241 to 7260) as described previously (48). The resultant 179-bp reverse transcriptase PCR products were purified by low-melting-point agarose gel electrophoresis and sequenced as described above.

Analysis of viral RNA synthesis. To study the effect of the mutations on RNA synthesis, the *Bss*HII-*Sal*I (nt 4238-MCS) fragments of the constructs were cloned in the chimeric subgenomic replicon pCB3/T7-LUC, in which the capsid coding P1 region is replaced by the firefly luciferase gene (45). Vero cells grown in 25-cm^2 flasks to a confluency of 75% were transfected with 4 μg of T7 RNA polymerase-generated pCB3/T7-LUC cRNA derived from *Sal*I linearized plasmids. The cells were washed three times with phosphate-buffered saline at 0, 4, 6, and 10 h after transfection and lysed in 400 μl of lysis buffer, and the luciferase activity was measured in a liquid scintillation counter, using the Luciferase Assay System according to the recommendations of the manufacturer (Promega).

In vitro translation reactions. Copy RNA transcripts were synthesized and translated in T7 TNT Rabbit Reticulocyte Lysate (Promega), a coupled transcription-translation system, according to the manufacturer's recommendations. The translation reactions (20 μl) were initiated with 0.5 μg of *Sal*I-linearized plasmid DNA and supplemented with 20% (vol/vol) HeLa cell initiation factors. Proteins were synthesized and labeled with 20 μCi of Tran-^{35}S-label (Amersham), which is a mixture of [^{35}S]cysteine and [^{35}S]methionine with a specific activity of >1,000 Ci/mmol, for 3 h at 30°C. After incubation, RNA was degraded by treatment with RNase T_1 (500 U) and RNase A (5 μg) for 10 min at 30°C. Translation products were analyzed with 5-μl amounts on a 12.5% polyacrylamide gel (Bio-Rad) containing sodium dodecyl sulfate (17). Gels were fixed in 30% methanol–10% acetic acid, rinsed in dimethyl sulfoxide, fluorographed using 20% PPO (2,5-diphenyloxazole) in dimethyl sulfoxide, dried under a vacuum, and exposed to Kodak XAR film at −80°C.

Three-dimensional model generation. A three-dimensional model was constructed using the SYBYL software (SYBYL Molecular Modelling Software, version 6.1A; Tripos, Inc., St. Louis, Mo.). Stacked domains were generated using default parameters for an "A" helical model (4). The initial model was optimized using energy minimizations (AMBER 3.0 all-atom force field [46] and charges, distance-dependent dielectric function, $\varepsilon_0 = 40$, 8 Å nonbonded cutoff, Powell minimizer with line searching) until the root mean square gradient converged to less than 0.05 kcal/Å^2. Neither counterions nor solvent molecules were added.

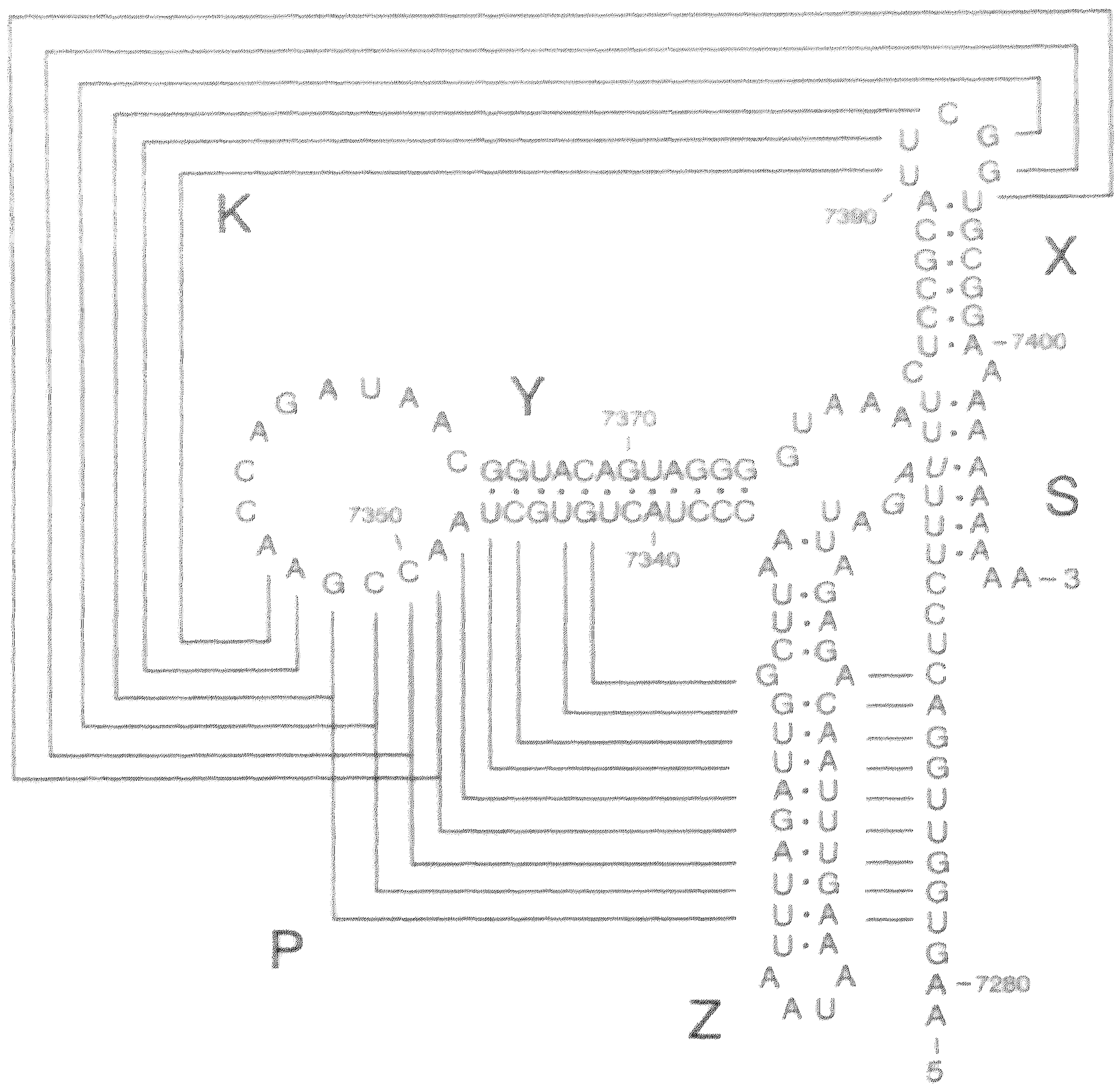

FIG. 1. Structure of coxsackie B3 virus 3′UTR. Shown is a model predicted by STAR. The 3′UTR consists of three hairpin structures indicated as X, Y, and Z. The Z hairpin is not present in the poliovirus-like enteroviruses. The structure is closed by the interaction of the poly(A) with a U stretch overlapping the 3′UTR and the 3D coding region, indicated as the S domain. The pseudoknot (P) and kissing (K) interactions between domain Y and the 3D polymerase coding region and domains X and Y, respectively, are represented by intercon-

dicating that it is double stranded. The flanking sequence in this hairpin loop (A_{7353}) showed a moderate single-stranded signal (Fig. 3A). Some subtle differences in the probing pattern of coxsackie B3 virus domain X compared to that obtained by the analysis described previously have been observed (27). These differences are due to the fact that in the previous report all single-strand-specific signals were indicated, very weak signals being marked by open symbols (27). In Fig. 3A, only strong and moderate signals are shown.

To verify the double-strand sensitivity of the hairpin loop of domain Y, we constructed pCB3-3′UTR:ACCG$_{7349-7352}$→UGGC by altering the double-strand-sensitive sequence in the loop of domain Y (CCG$_{7350-7352}$) to the complementary bases (Fig. 3B). This construct showed sensitivities to single- and double-stranded probes, as did the wild-type sequence, except that the double-strand-sensitive sequence in the hairpin loop of the Y domain now showed a very strong sensitivity for

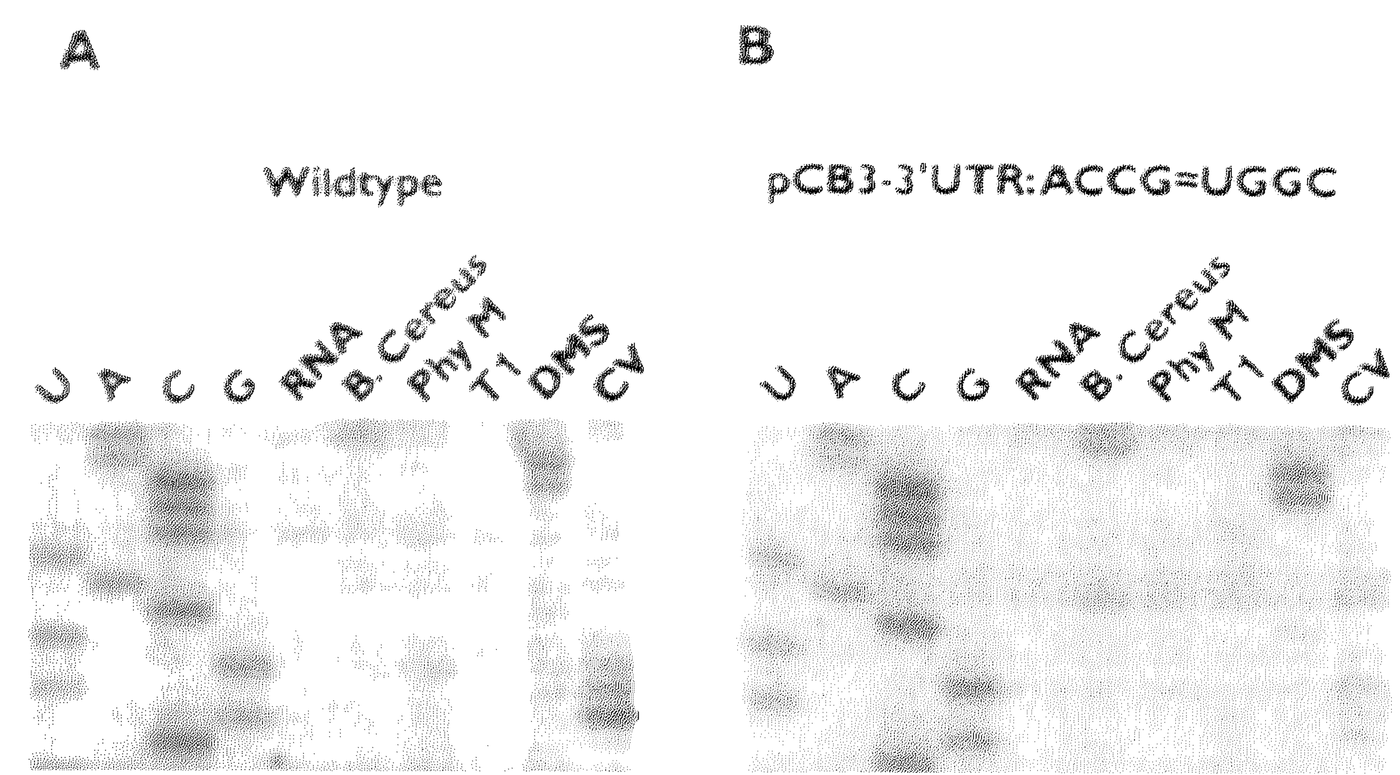

necting lines. The stop codon is shown in italics.

RESULTS

Models of the 3′UTR of coxsackie B3 virus. The structure of the 3′UTR of different enteroviruses was predicted by STAR. The 3′UTR is highly conserved, and based on the size of the 3′UTR, the enteroviruses can be divided into a poliovirus-like subgroup containing 65 nt and a coxsackie B virus-like subgroup that is approximately 100 nt long. Both enterovirus subgroups possess two common domains that can both form a stem-loop structure (domains X and Y [Fig. 1]). The coxsackie B virus-like subgroup contains a third domain (domain Z [Fig. 1]), located upstream of domain Y, that is also capable of forming a stem-loop, resulting in a final secondary structure that looks like a cloverleaf (Fig. 1). All enteroviruses contain a short poly(U) stretch prior to the termination codon. This poly(U) stretch can base pair with residues from the poly(A) tract and, hence, form element S (Fig. 1). An interaction between domain Y (nt 7343 to 7352) and sequences within the 3D coding region (nt 7282 to 7290), forming a classical pseudoknot structure, and another interaction between the same region in the loop of domain Y (nt 7349 to 7354) and the loop of domain X (nt 7390 to 7395), forming a loop-loop intramolecular "kissing" RNA interaction, appeared to be possible (Fig. 1). In contrast to the pseudoknot, the kissing interaction is limited to the 3′UTR. The model could be employed for all enteroviruses sequenced so far, indicating that it is phylogenetically conserved as well (data not shown).

The model was experimentally verified, using probes specific for single- and double-stranded RNA regions (Fig. 2). The results obtained with the enzymatic and chemical probing were in reasonable accord with the predicted secondary structure of the model (Fig. 3). Concerning the tertiary structural elements, the $CCG_{7350-7352}$ stretch in the loop of domain Y indeed showed a strong sensitivity for cobra venom nuclease V_1, in-

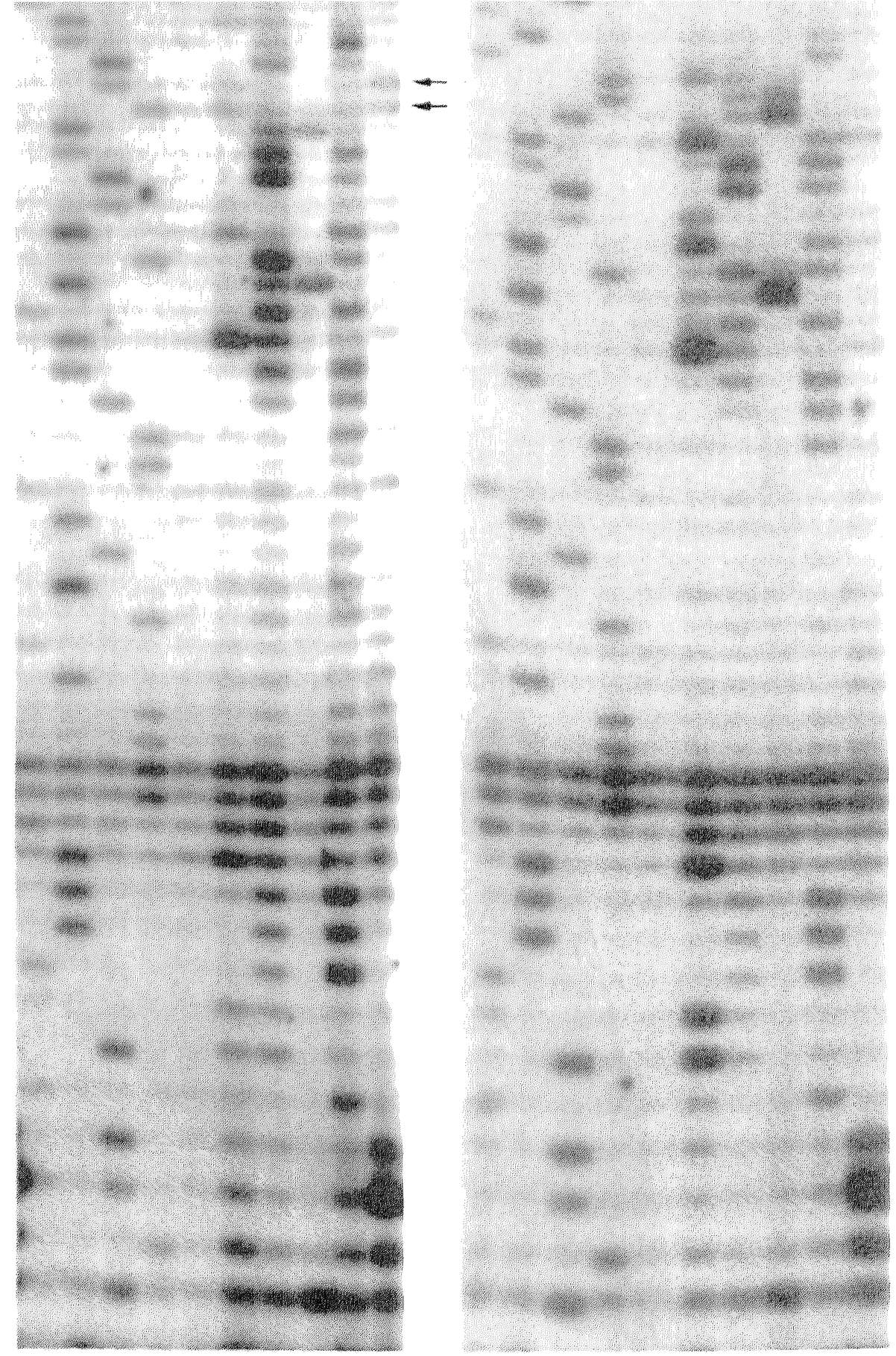

FIG. 2. Chemical and enzymatic probing of the coxsackie B3 virus 3′UTR. The virus RNAs were treated with *B. cereus*, *Phy M*, RNase T_1 (T1), DMS, and cobra venom nuclease V_1 (CV) as described in Materials and Methods, and then they were used as templates for the oligonucleotide-primed cDNA synthesis by reverse transcriptase. Lane RNA corresponds to the nontreated RNA samples. Lanes G, C, A, and U correspond to the samples containing untreated RNA templates and appropriate terminators for DNA synthesis. (A) Part of the primary data obtained by the probing of the wild-type virus; (B) part of construct pCB3-3′UTR:$ACCG_{7349-7352}$→UGGC.

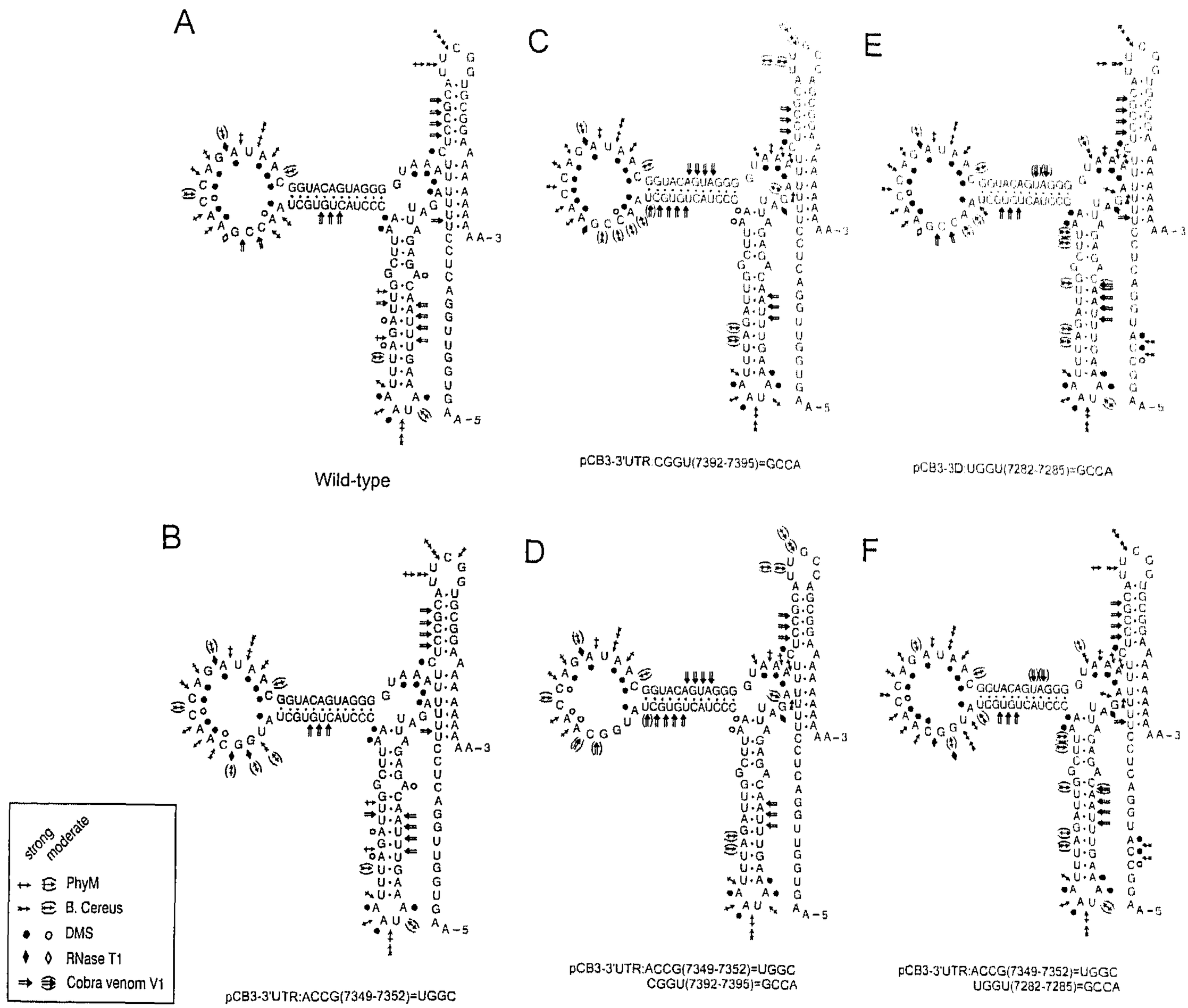

FIG. 3. Chemical and enzymatic verification of the predicted structure of coxsackie B3 virus 3′UTR. RNase T_1 (attacking single-stranded regions), *Phy M* (cleaving after A and U), and *B. cereus* (cleaving after U and C) as well as DMS served as probes for single strandedness, while cobra venom nuclease V_1 cleaved double-stranded RNA helical regions. The positions of cleavages or modifications induced by single- or double-stranded probes are indicated by symbols explained in the figure. Relatively moderate signals are represented by open and bracketed symbols. Illustrated are compositions from several independent experiments. (A) Wild-type coxsackievirus B3 structure; (B) construct pCB3-3′UTR:$ACCG_{7349-7352}$→UGGC; (C) construct pCB3-3′UTR:$CGGU_{7392-7395}$→GCCA; (D) construct pCB3-3′UTR:$ACCG_{7349-7352}$→UGGC/$CGGU_{7392-7395}$→GCCA; (E) construct pCB3-3D:$UGGU_{7282-7285}$→GCCA; (F) construct pCB3-3′UTR:$ACCG_{7349-7352}$→UGGC/$UGGU_{7282-7285}$→GCCA. Further details are described in the text.

single-stranded probes, suggesting that the tertiary interaction was being disturbed by this mutation. To gain insight into the origin of the tertiary structure, we constructed pCB3-3′UTR:$CGGU_{7392-7395}$→GCCA, in which the CGGU nucleotide stretch in the loop of domain X was replaced by its complementary sequence, disturbing the possible kissing interaction. Chemical and enzymatic probing of the copy RNA of this construct gave the same results as those obtained with pCB3-3′UTR:$ACCG_{7349-7352}$→UGGC, and the double-stranded region in the loop of domain Y became sensitive for single-stranded probes (Fig. 3C). The double mutation in construct pCB3-3′UTR:$ACCG_{7349-7352}$→UGGC/$CGGU_{7392-7395}$→GCCA fully restored the possible kissing interaction and indeed restored the double-strand-sensitive nature of the $CCG_{7350-7352}$ sequence in the loop of domain Y (Fig. 3D). In pCB3-3D:$UGGU_{7282-7285}$→GCCA, the sequence in the 3D coding region is altered such that a possible pseudoknot is fully disturbed. This mutation, however, had no effect on the double-strand nature of the $CCG_{7350-7352}$ sequence in the loop-sensitive of domain Y, arguing against a tertiary interaction between the loop in domain Y and the sequences within the RNA polymerase coding region (Fig. 3E). The double-mutated pCB3-3′UTR:$ACCG_{7349-7352}$→UGGC/$UGGU_{7282-7285}$→GCCA did not further affect the probing results (Fig. 3F).

Experimental verification of the pseudoknot interaction. To verify the existence of a pseudoknot interaction between domain Y (G_{7343}–G_{7352}) and the 3D polymerase coding region (U_{7282}–C_{7291}), two mutations were induced and introduced in the infectious cDNA clone pCB3/T7. Construct pCB3-3′UTR:$GUGC_{7343-7346}$→$CAGG/GUAC_{7365-7368}$→CUUG creates a mirror image of the top part of the Y stem and should disturb the interaction with the 3′ end of the 3D polymerase coding region, and construct pCB3-3D:$UUG_{7285-7287}$→CUU, in which the leucine codon UUG in the 3D polymerase coding region was replaced by the leucine codon CUU, should disturb the

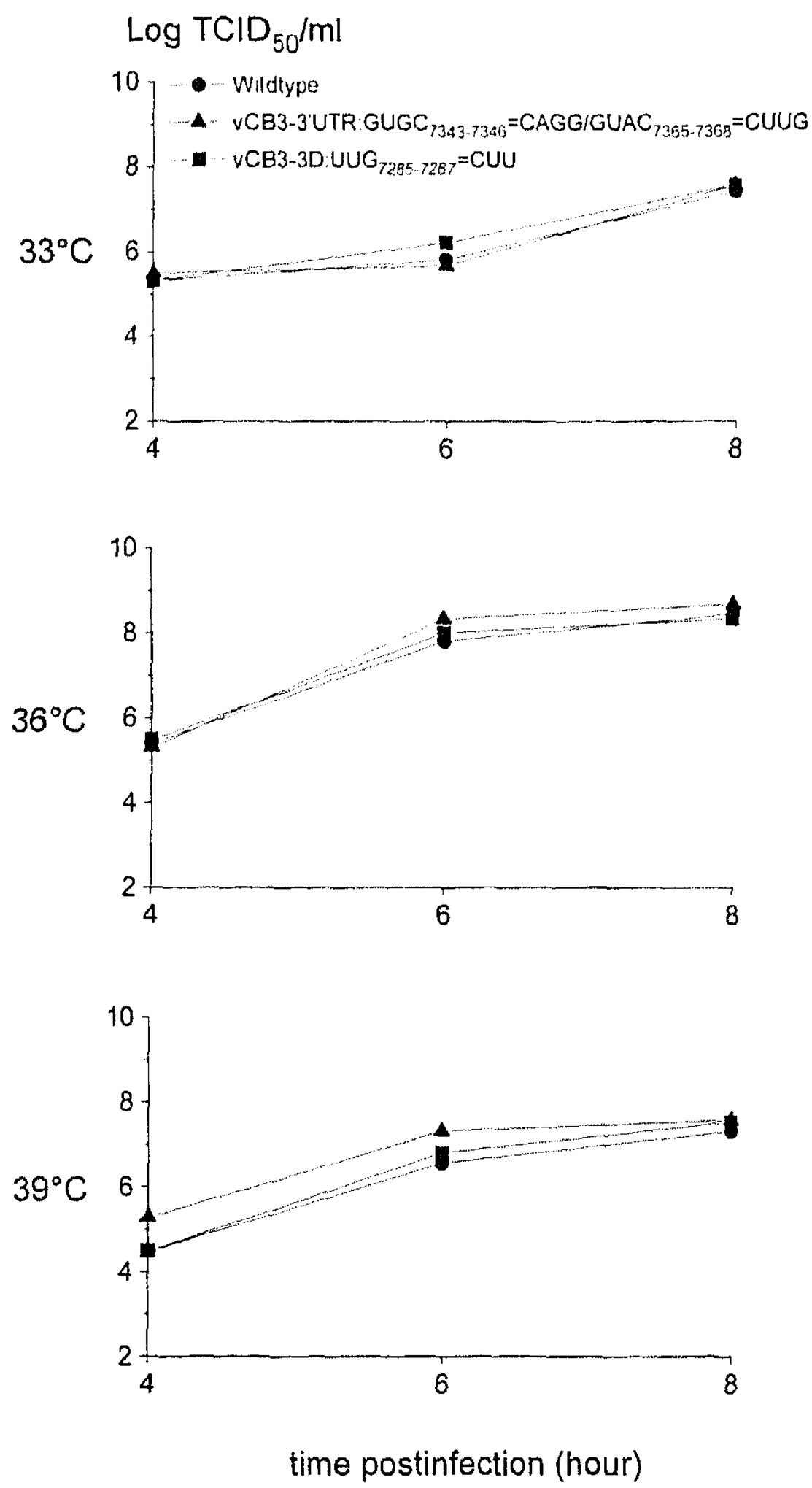

FIG. 4. Single-cycle growth curves of the mutants involved in the pseudoknot interaction. Vero cells were infected with wild-type and mutant viruses at an MOI of 1 $TCID_{50}$ per cell. The cells were grown at 33, 36, and 39°C for 4, 6, and 8 h. Virus titers were determined as described in Materials and Methods. The mutant viruses are indicated in the figure.

formation of the pseudoknot while the 3D polymerase amino acid sequence remains intact. The effect of the mutations on virus viability was studied by transfection of Vero cells with copy RNA transcripts. A CPE was observed with both mutants at 48 to 72 h after transfection, which is similar to that obtained with wild-type pCB3/T7. Moreover, both mutations yielded virus which exhibited the growth characteristics of wild-type virus, as examined by single-cycle growth analysis at 33, 36 and 39°C (Fig. 4). Sequence analysis of the 3D polymerase–3′UTR region of these mutant viruses showed that the mutations introduced by site-directed mutagenesis were retained in the viral RNA and that no other mutations had occurred. These results are in accordance with those from the chemical and enzymatic probing, and therefore, no evidence was found for the presence of this pseudoknot interaction.

Experimental verification of the kissing interaction. To investigate the existence of a kissing interaction, further site-specific mutations were introduced. Constructs pCB3-3′UTR:G_{7352}→C and pCB3-3′UTR:C_{7392}→G disturbed the tertiary interaction, resulting in no virus being produced after transfection (and passage) of the copy RNAs of these mutations to Vero cells at either 33 or 36°C. When both mutations were generated simultaneously to yield pCB3-3′UTR:C_{7392}→G/G_{7352}→C, the tertiary interaction was restored and the virus obtained exhibited the growth characteristics of the wild-type virus, as examined by single-cycle growth analysis at 33, 36, and 39°C (Fig. 5). Replacing the cytosine at position 7392 with uracil yielded pCB3-3′UTR:C_{7392}→U, in which a U_{7392}/G_{7352} base pair in the tertiary interaction was generated, which proved unstable and resulted in a temperature-sensitive virus (Fig. 5). Replacing the G_{7352} with adenosine in construct pCB3-3′UTR:G_{7352}→A led to an A_{7352}/C_{7392} mismatch in the tertiary interaction which proved lethal. Introducing both substitutions in construct pCB3-3′UTR:C_{7392}→U/G_{7352}→A restored the interaction and generated a viable but temperature-sensitive virus which exhibited growth characteristics similar to those of virus vCB3-3′UTR:C_{7392}→U (Fig. 5). Two further mutations were introduced to investigate the importance of the A_{7353}/U_{7391} base pair in which the adenosine showed a moderate single-strand sensitivity (Fig. 3). Both constructs pCB3-3′UTR:U_{7391}→G and pCB3-3′UTR:A_{7353}→C disturbed the tertiary interaction and resulted in viable but temperature-sensitive viruses (Fig. 5). The double mutation in construct pCB3-3′UTR:U_{7391}→G/A_{7353}→C restored the interaction, and the resulting virus exhibited growth characteristics similar to those of the wild-type virus (Fig. 5). Sequence analysis of the 3′UTR of these mutant viruses showed that the mutations introduced by site-directed mutagenesis were retained in the viral RNA and that no other mutations had occurred. The results obtained by the mutagenic analysis are in accordance with the probing results. Thus, an RNA-RNA tertiary interaction exists between the hairpin loops X and Y, forming an intramolecular kissing interaction which is essential for virus reproduction.

Biological function of the kissing interaction in virus reproduction. In vitro translation reactions were performed to investigate whether the mutations affected translation or processing of the polyprotein. Figure 6 shows that the protein patterns obtained with the mutated constructs were similar to those of the wild-type virus, indicating that disturbing the kissing interaction caused no defects in the synthesis and processing of the virus polyprotein.

In a previous study (45), a chimeric subgenomic replicon, pCB3/T7-LUC, which carries the luciferase gene in place of the P1 capsid protein coding region, was constructed and used to study the effects of mutations on RNA replication. After transfection of pCB3/T7-LUC copy RNA, a triphasic pattern of luciferase accumulation that reflects virus RNA replication can be observed. First, luciferase activity increases as the result of translation of the input copy RNA (phase I); then the activity remains constant until the fifth hour after transfection in which replication occurs (phase II); and finally, the activity shows a second increase as a result of the translation of newly synthesized chimeric RNA strands (phase III). Figure 7 shows this triphasic pattern after transfection of wild-type pCB3/T7-LUC. A similar pattern was obtained with construct pCB3-3′UTR/T7-LUC:$GUGC_{7343-7346}$→$CAGG/GUAC_{7365-7368}$→CUUG, in which the pseudoknot was disturbed although the virus obtained showed wild-type growth characteristics, and with construct pCB3-3′UTR/T7-LUC:C_{7392}→G/G_{7352}→C, in which the kissing interaction was restored. To study whether some of the mutations in the 3′UTR were lethal because of a replication defect, the mutations were introduced in the rep-

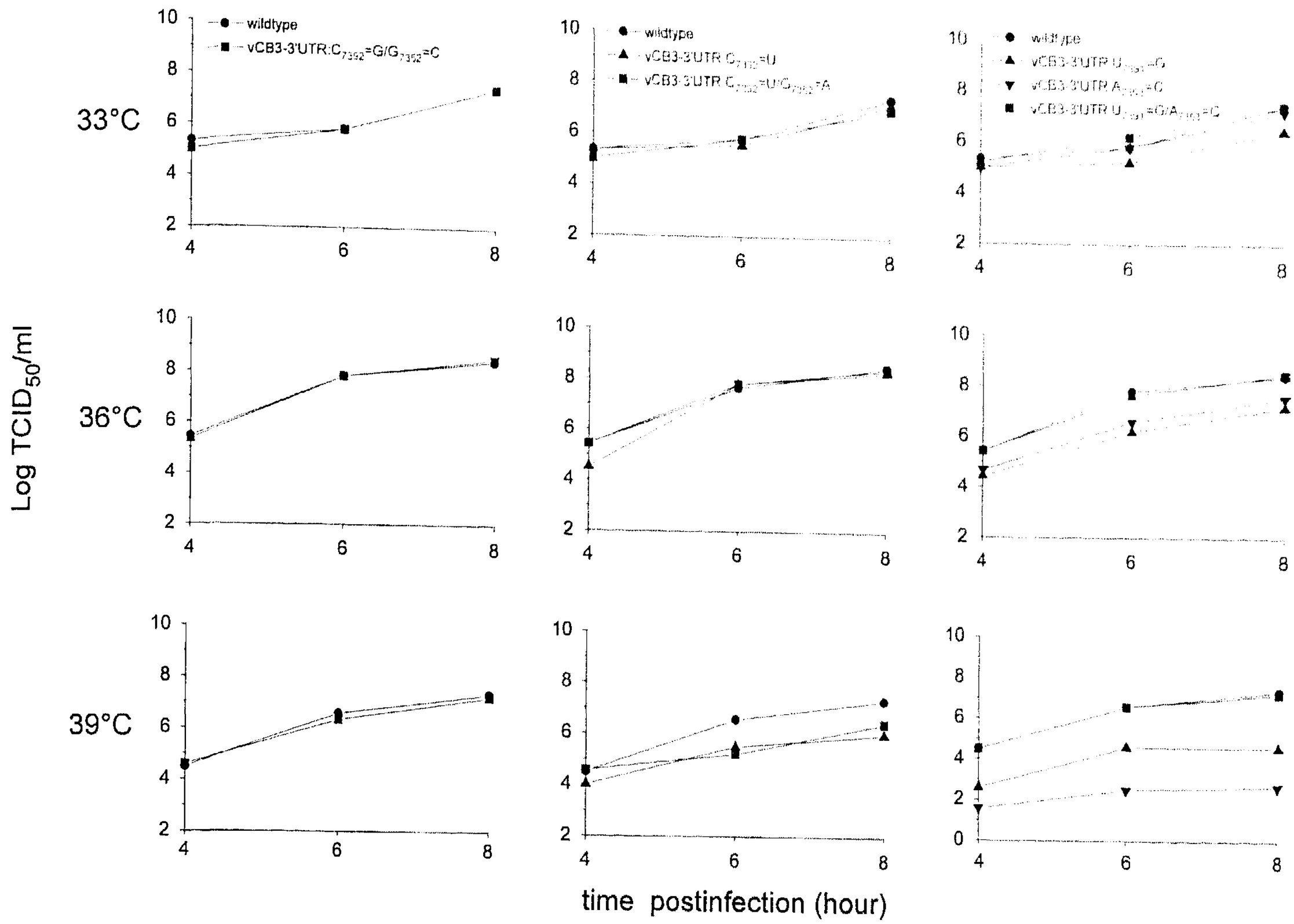

FIG. 5. Single-cycle growth curves of the mutants involved in the kissing interaction. Vero cells were infected with wild-type and mutant viruses at an MOI of 1 $TCID_{50}$ per cell. The cells were grown at 33, 36, and 39°C for 4, 6, and 8 h. Virus titers were determined as described in Materials and Methods. The mutant viruses are indicated in the figure.

licon, and copy RNA of the mutated replicons was transfected to Vero cells. Figure 7 shows that disturbing the kissing interaction had a primary effect on virus replication, as was demonstrated by the complete absence of the third phase. These data show that the kissing interaction between the X and Y domains of the coxsackie B3 virus 3′UTR plays a pivotal role in the replication of the virus.

Three-dimensional model of the coxsackie B3 virus 3′UTR. According to the secondary structure model, the domains X and S can be regarded as having one common stacked helical element forming a helical superdomain (Fig. 1 and 8). Since there are no intervening nucleotides between domains Y and Z, the helical characteristics of the respective domains can also be stacked, forming a second helical superdomain. The kissing interaction, or K domain, comprising 6 base pairs, can be stacked as a continuation of either one of the helical superdomains. An initial model in which the kissing interaction was an elongation of the Y and Z domains proved unstable, and further efforts were made, using the model in which the K domain is an uninterrupted connection to the X-S helical superdomain (Fig. 8). Residue A_{7391} was used to fold back from the K domain to the X domain, bridging the major groove of the extended helix S-X-K. The two stacked moieties were joined via residue A_{7348} and oriented relative to one another using the 9-nt stretch sequence C_{7355} to C_{7363} to fill the gap between the K and Y domains. Simultaneously, constraints were satisfied to allow A_{7298}–U_{7301} and G_{7376}–A_{7380} to connect both helical superdomains. The three-dimensional model presented in Fig. 9 shows the results after optimization using energy minimization.

DISCUSSION

The enteroviruses can be divided into two main groups according to serological tests and genetic analysis, one subgroup containing the polioviruses and most coxsackie A viruses and the other consisting of coxsackie B viruses, enterovirus 71, the echoviruses, and some coxsackie A viruses (5, 49). With respect to the 3′UTR, the poliovirus-like subgroup was found to have an approximately 28-nt deletion, representing a full hairpin structure, when compared to members of the coxsackie B virus-like subgroup. As also found in this study, the secondary structures predicted for the enterovirus 3′UTR all seem to point to a conformation consisting of two or three stem-loops (domains X, Y, and Z), in which part of the poly(A) tract is included (domain S) (5, 13, 27). The model we employed was based on a calculation of the thermodynamics and appeared to be similar to that described by Pilipenko et al. (27), in which a phylogenetic comparison was used for the RNA folding. Minor differences were predicted in the stem of domain Z, the corresponding multibranched loop, and the size of the stem of domain X. Minor differences were also predicted between the model described here and that developed by Jacobson et al. (13), who also used a thermodynamic approach. However, the fact that each group independently proposed the same secondary structure for the enterovirus 3′UTR makes the actual ex-

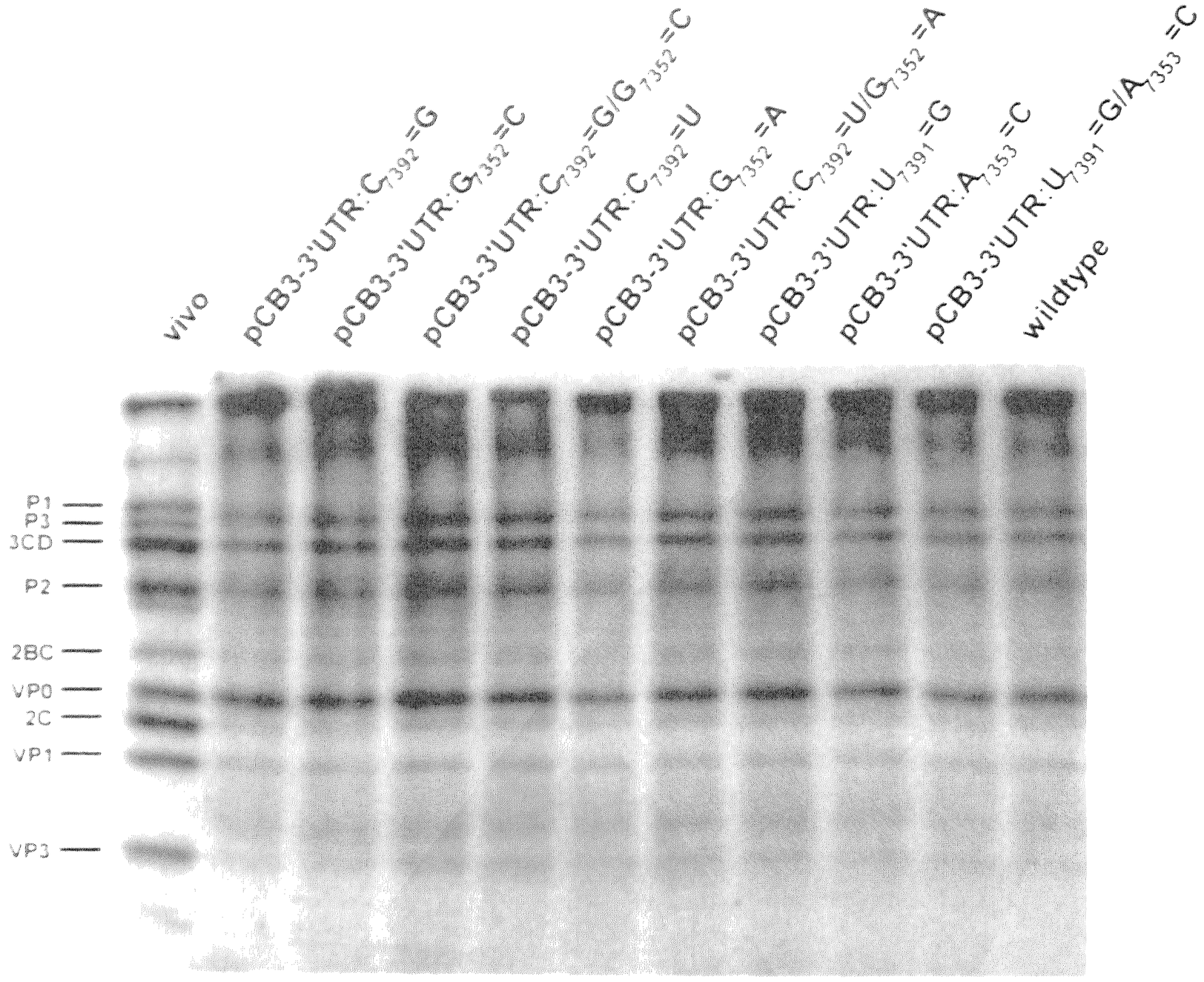

FIG. 6. In vitro translation of RNA derived from wild-type pCB3/T7 and the 3′UTR mutated plasmids. In vitro translation was assayed in a T7 TNT-coupled transcription-translation reticulocyte lysate system supplemented with HeLa S10 extract (see Materials and Methods). The mutated constructs are indicated in the figure. An extract from wild-type infected cells, pulse-labeled with [^{35}S]methionine, was used as a marker (lane vivo). The positions of proteins and precursors are indicated on the left.

istence of this structure plausible. Indeed, chemical and enzymatic probing of the 3′UTR was in reasonable agreement with the predicted secondary structure.

Two alternative structures were possible for the tertiary structure of the enterovirus 3′UTR. In the first one, a classical pseudoknot structure (29) in which bases of domain Y would pair with nucleotides located upstream in the 3D polymerase coding region is formed, whereas the second predicted a loop-

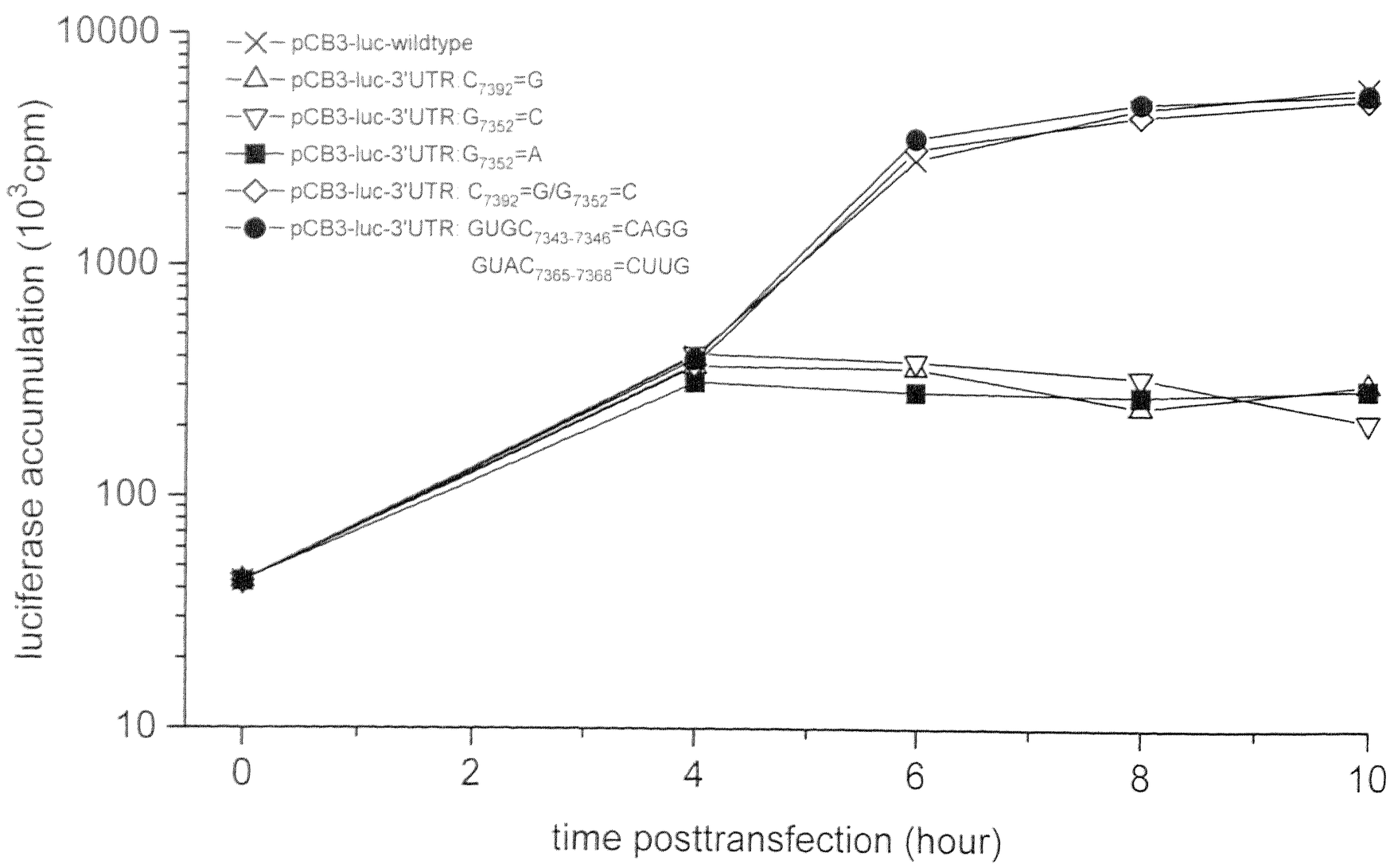

FIG. 7. Analysis of RNA replication of 3′UTR mutations with a chimeric luciferase replicon pCB3/T7-LUC. Shown is the luciferase accumulation after transfection of Vero cells with copy RNA of wild-type pCB3/T7-LUC, pCB3-3′UTR/T7-LUC:GUGC$_{7343-7346}$→CAGG/GUAC$_{7365-7368}$→CUUG and pCB3-3′UTR/T7-LUC: C$_{7392}$→G/G$_{7352}$→C. No phase III luciferase accumulation was observed in the pCB3/T7-LUC constructs containing those 3′UTR mutations that were lethal upon transfections. Luciferase activities were measured as described in Materials and Methods.

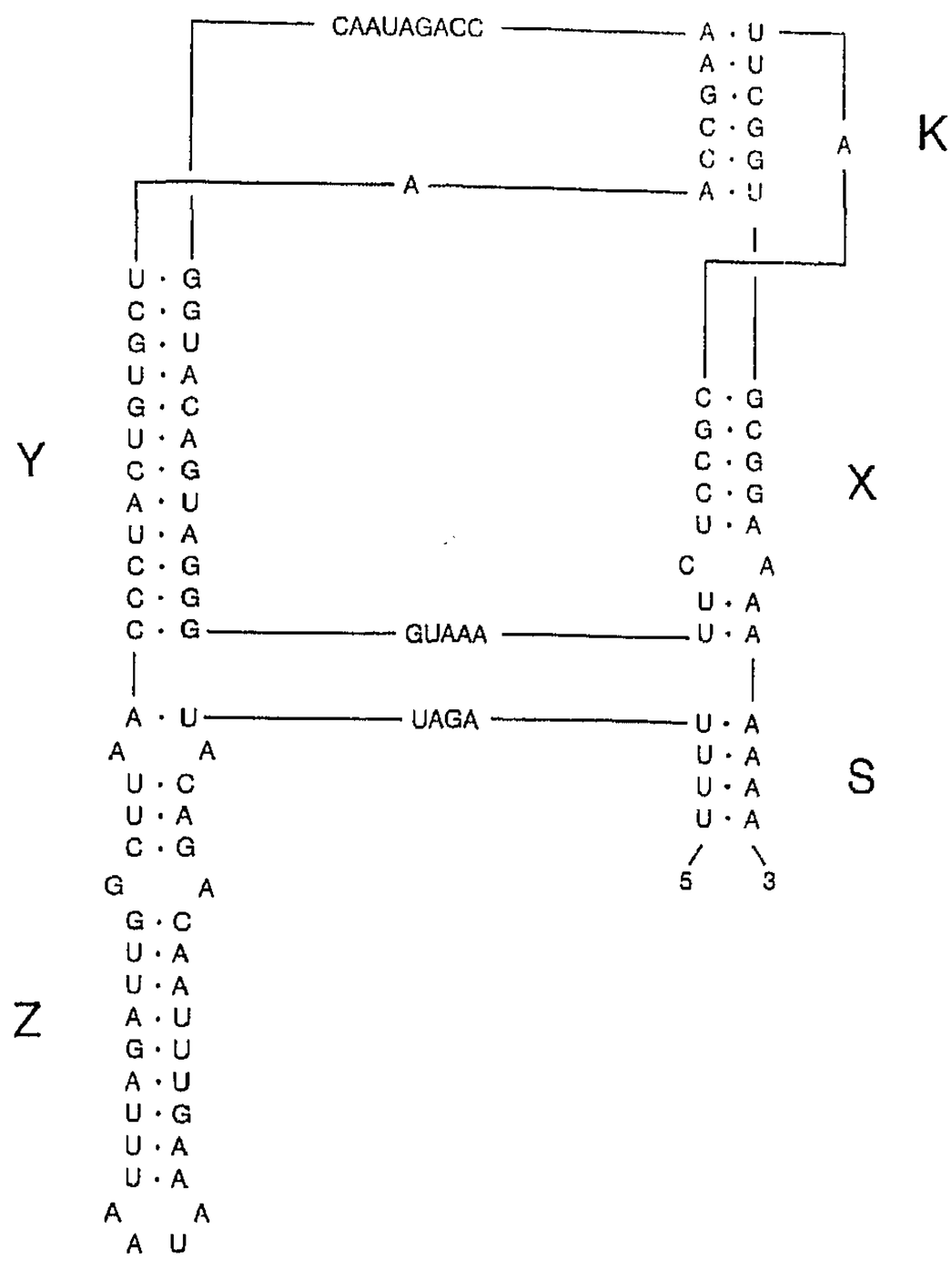

FIG. 8. Tertiary structure model of the coxsackie B3 virus 3′UTR. The specific domains X, Y, Z, and S are indicated as shown in Fig. 1. The K domain represents the kissing interaction. For further details, see the text.

loop intramolecular kissing interaction between nucleotides in the loop structure of domain Y and domain X. Using mutational analysis, Pierangeli et al. (24) also suggested the existence of a tertiary interaction in the 3′UTR, although they were not able to locate this specific interaction. Although the nucleotide stretch ($ACCG_{7349-7352}$) in domain Y is single stranded in the secondary structure model, it showed sensitivity for the double-strand-specific cobra venom nuclease V1 or only moderate single-stranded hits by chemical and enzymatic probing, indicating its involvement in tertiary base pairing. When this double-strand-sensitive region was replaced in the loop of domain Y with the complementary sequence (construct pCB3-3′UTR:$ACCG_{7349-7352}$→UGGC), it showed a very strong sensitivity for single-stranded probes. Replacing the possible interacting bases in the loop of domain X with the complementary sequence (construct pCB3-3′UTR: $CGGU_{7392-7395}$→GCCA) also resulted in a strong sensitivity for single-stranded probes of the $CCG_{7350-7352}$ stretch in the loop of domain Y. In the double mutation, the kissing interaction was restored, and probing this construct indeed restored the double-strand sensitivity of the $CCG_{7350-7352}$ stretch in the loop of domain Y. The absence of cobra venom nuclease V_1-induced cleavages in the loop of domain X may be due to the limitations of the method. In fact, V_1 RNase does not induce cleavages in all double-stranded regions (Fig. 3A). Digestion with single-stranded-specific probes in the loop sequence of domain X may be due to two reasons. (i) There is an equilibrium between two spatial foldings (with and without the kissing interaction). Thus, the single-stranded signals appeared when the tertiary structure is in the second state. (ii) These observed signals are the secondary cleavages. When the primary single-strand-specific cleavage occurs in the loop of domain Y, two RNA molecules may disperse. Hence, the kissing interaction may be destabilized, resulting in the observed single-stranded signals. Construct pCB3-3D:$UGGU_{7282-7285}$→GCCA, in which the 3D coding sequence involved in a possible pseudoknot interaction was replaced with the complementary sequence, did not affect the double-stranded nature of the corresponding sequence in the loop of domain Y. Also, the double-stranded nature of the nucleotide stretch $CCG_{7350-7352}$ was not restored in pCB3-3′UTR:$ACCG_{7349-7352}$→UGGC/ $UGGU_{7282-7285}$→GCCA. A kissing interaction between the hairpin loops of Y and X rather than a pseudoknot interaction between hairpin loop Y and sequences in the 3D coding region is therefore favored. This is in contrast to the findings of Jacobson et al. (13), who described experimental evidence for the existence of such a pseudoknot interaction in the poliovirus 3′UTR using a temperature-sensitive mutant (3NC202), isolated previously by Sarnow et al. (36), which has an 8-nt insertion within the loop of domain Y, directly downstream of the stem structure. The mutant 3NC202 showed wild-type levels of virus yields at a low temperature and decreased yield when grown at 39.5°C. They subsequently isolated eight revertants that synthesized wild-type levels of RNA at 39.5°C, of which six could reform a wild-type pseudoknot structure. However, this cannot be considered proof for such a structure, since mutant 3NC202 itself was capable of forming a pseudoknot structure that was almost identical to the wild-type structure (13). Therefore, we constructed pCB3-3′UTR:$GUGC_{7343-7346}$→CAGG/ $GUAC_{7365-7368}$→CUUG to create a mirror image of the top part of the Y stem and disturbed the interaction with the 3′ end of the 3D polymerase coding region, and we also generated pCB3-3D:$UUG_{7285-7287}$→CUU, in which the leucine codon CUU in the 3D coding region replaced UUG and succeeded in disturbing the formation of the pseudoknot while keeping the 3D amino acid sequence intact. Both mutants yielded a virus which exhibited growth characteristics identical to those of the wild-type virus. We therefore could find no evidence to support the presence of this pseudoknot interaction. This is in agreement with the results described by Rohll et al. (34) and Pierangeli et al. (24), who found that insertions (up to 1,000 nt) just downstream of the termination codon, resulting in a very low probability to form a pseudoknot, did not influence the RNA replication of the virus RNA. The kissing interaction showed a remarkable resemblance to the tertiary structure predicted by Pilipenko et al. (27), which was based on phylogenetic comparisons. Our experimental evidence suggest that a kissing interaction between the loop structures of domains X and Y does indeed exist. Replacement of the double-strand-sensitive G_{7352} in the loop of domain Y with a cytosine (pCB3-3′UTR:G_{7352}→C) introduced a C_{7352}/C_{7392} mismatch and a disturbance of the kissing interaction. This mutation appeared to be lethal. Replacement of the complementary C_{7392} in the loop of the X domain with a guanosine (pCB3-3′UTR: C_{7392}→G) also resulted in a lethal mutation. However, when both mutations were introduced simultaneously (pCB3-3′UTR:C_{7392}→G/G_{7352}→C), the kissing interaction was restored and the resultant virus exhibited the growth characteristics of the wild-type virus. When the cytosine at position 7392 was replaced with uracil, a U_{7392}/G_{7352} base pair was generated in the kissing interaction, resulting in a temperature-sensitive virus which could produce only 5% of the wild-type virus yield at 39°C, most probably due to the less stable U/G base pairing (39). Replacement of the complementary G_{7352} in the loop of domain Y into an adenosine, resulting in an A_{7352}/C_{7392} mismatch in the kissing interaction, also proved to be lethal. The simultaneous introduction of both mutations, resulting in

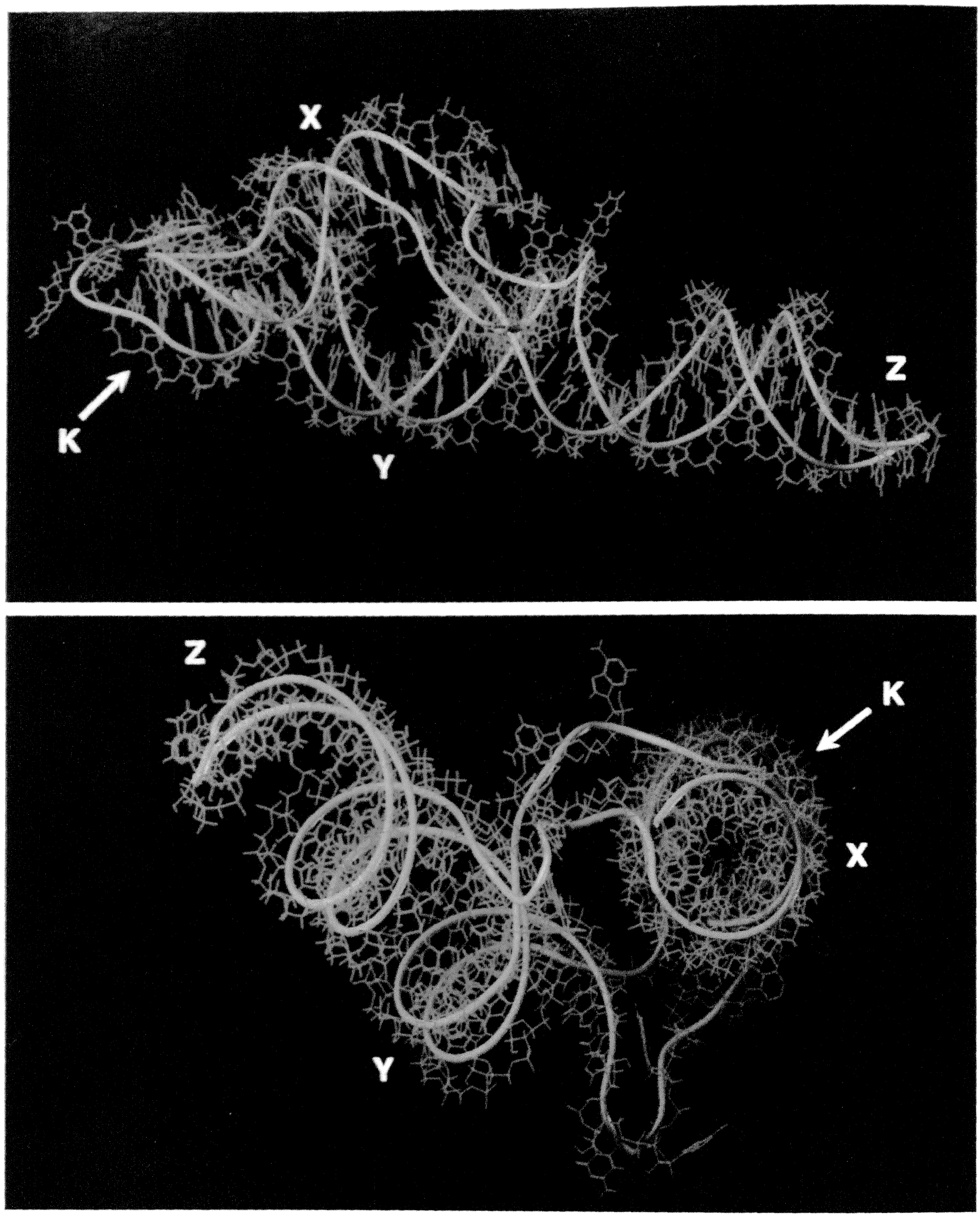

FIG. 9. Three-dimensional model of the coxsackie B3 virus 3′UTR. Shown are stick diagram displays from the side view of the model (top) and from the top view of the coxsackie B3 virus 3′UTR (bottom).

pCB3-3′UTR:C_{7392}→U/G_{7352}→A, produced a viable but temperature-sensitive virus and at 39°C yielded only 13% of that produced by the wild-type virus. The growth characteristic of this latter mutant is similar to that of mutant vCB3-3′UTR: C_{7392}→U and might be accounted for by similar stabilities of U/G and A/U base pair interactions (39). The importance of the moderately single-strand-sensitive A_{7353} in the loop of domain Y was studied in pCB3-3′UTR:A_{7353}→C and pCB3-3′UTR:U_{7391}→G. Both mutations produced temperature-sensitive viruses with virus yields of 0.002 and 0.2% of that of wild-type virus at 39°C, respectively. When both mutations were introduced simultaneously, the resultant mutant virus had wild-type virus growth characteristics at 39°C, clearly indicating that this base pair is involved in the kissing interaction as well.

The full characterization of the kissing interaction is now in progress. We assume that it consists of six base pairs, which is also phylogenetically acceptable, since it can be applied to all enteroviruses sequenced so far (data not shown). Furthermore,

six residues are essential to have residue A_{7391} to gap the major groove of the superdomain and fold back from domain K to domain X (Fig. 8). Based on these findings, we constructed a three-dimensional model of the 3′UTR using computer assisted molecular modelling (Fig. 9). Pilipenko et al. (27) proposed that the final three-dimensional structure of the 3′UTRs of the poliovirus-like and coxsackie B virus-like subgroups were similar in their overall organization to tRNA species. Indeed, a tRNA-like conformation of the 3′UTR has earlier been found in some alpha-like RNA plant viruses (32, 33). However, these virus RNAs can be aminoacylated (19), a feature that is unknown for the 3′UTR of enteroviruses. Comparisons of the three-dimensional structure of the enterovirus 3′UTR with the crystallographic structures of tRNA molecules (16, 40) showed that the structures were dissimilar (data not shown), since the enterovirus 3′UTR does not have the typical L-shaped formation found in tRNA (Fig. 9). Disruption of the tertiary interaction had no effect on virus translation and processing, since wild-type protein patterns were found using an in vitro translation assay. However, disturbing the kissing interaction resulted in a defect in virus RNA replication, as was demonstrated with a subgenomic coxsackie B3 virus replicon. Very recently, it has been demonstrated that in the poliovirus 3′UTR, an intramolecular kissing interaction is also essential for virus replication (28).

The importance of RNA structures in RNA-protein interactions is generally known, and the tertiary RNA structure can be essential for stabilizing the structure for the subsequent interaction with proteins (11). As in the case of other complex higher-order RNA structures like pseudoknots, it is reasonable to assume that the kissing interaction in the enterovirus 3′UTR acts as a specific binding site for viral and/or cellular proteins involved in the initiation of negative-strand RNA synthesis (23, 42). Indeed, Harris et al. (12) have described the formation of a 3′-terminal ribonucleoprotein complex composed of a 3AB-3CD interaction with the 3′UTR. The subsequent proteolysis of $3CD^{pro}$ releases the 3D polymerase. Protein 3AB then forms a complex with protein 3D to stimulate the activity of the virus polymerase (12, 18, 30), which may use the uridylated VPg (44) to initiate negative-strand RNA synthesis. A similar protein 3D interaction with a tertiary (pseudoknot) structure in the 3′UTR of encephalomyocarditis virus has also been proposed (10). Our results suggest that the kissing interaction most probably forms the binding site and not the pseudoknot structure, as suggested by Harris et al. (12). Although Harris et al. (12) did not consider other proteins to contribute to the complex formation, Todd et al. (43) recently provided evidence for an interaction of the 3′UTR with certain unidentified cellular proteins as well. We propose that the kissing interaction is the essential structural feature of the origin of replication required for its functional competence in virus negative-strand RNA synthesis.

The presence of such a tertiary structure in the 3′UTRs of both the coxsackie B virus- and poliovirus-like viruses makes the exchange of the 3′UTR between these viruses and the subsequent replication of the chimeras understandable, since the binding sites are identical (34). On the other hand, the rhinovirus genus has a 3′UTR which consists of a single stem-loop structure which cannot form a kissing interaction. However, a poliovirus chimera containing the rhinovirus 14 3′UTR was still capable of initiating poliovirus negative-strand RNA synthesis (34), which is difficult to explain. One explanation might be that this occurs because ribonucleoprotein complex formation occurs differently in the rhinovirus 3′UTR, although formation of the complex as such is sufficient to initiate replication. Rohll et al. (34) also found replication in a poliovirus replicon containing the hepatitis A virus 3′UTR, which is also unable to form a kissing structure. However, these results could not be confirmed in vivo using a full-length infectious poliovirus cDNA clone containing the hepatitis A virus 3′UTR (23).

An intermolecular kissing interaction has also been postulated to describe the mechanism of antisense RNA-target RNA duplex formation for the replication control of plasmid R1 (20–22). Hitherto, the existence and biological importance of an intramolecular kissing interaction between two RNA hairpin loops has only been postulated to take place in a variety of RNA molecules such as signal recognition particle RNA (50), *Escherichia coli* 4.5S RNA (38), archaebacterial 7S RNA (14), and also in human immunodeficiency virus (8). We have now demonstrated that these interactions do exist and might even be a general feature in the higher-order structures of RNA that are essential for it to function effectively.

ACKNOWLEDGMENTS

We thank Reinhard Kandolf, University of Tübingen, Germany, for his generous gift of the infectious coxsackie B3 virus clone pCB3/T7, J. Flanagan, University of Florida, for the HeLa cell initiation factors, and Peter Donnelly, for critically reviewing the manuscript.

This research was partly supported by grants from the European Communities (INTAS/RFBR no. 01365.i96), the International Science Foundation, the Human Frontiers Science Program Organization, and the Russian Foundation for Basic Research to Vadim I. Agol.

REFERENCES

1. **Abrahams, J. P., M. van den Berg, E. van Batenburg, and C. Pleij.** 1990. Prediction of RNA secondary structure, including pseudoknotting, by computer simulation. Nucleic Acids Res. **18:**3035–3044.
2. **Andino, R., G. E. Rieckhof, and D. Baltimore.** 1990. A functional ribonucleoprotein complex forms around the 5′-end of poliovirus RNA. Cell **63:**369–380.
3. **Andino, R., G. E. Rieckhof, P. L. Achacoso, and D. Baltimore.** 1993. Poliovirus RNA synthesis utilizes an RNP complex formed around the 5′-end of viral RNA. EMBO J. **12:**3587–3598.
4. **Arnott, S., D. W. L. Hukins, and S. D. Dover.** 1972. Optimised parameters for RNA double-helices. Biochem. Biophys. Res. Commun. **48:**1392–1399.
5. **Auvinen, P., G. Stanway, and T. Hyypiä.** 1989. Genetic diversity of enterovirus subgroups. Arch. Virol. **104:**175–186.
6. **Bienz, K., D. Egger, T. Pfister, and M. Troxler.** 1992. Structural and functional characterization of the poliovirus replication complex. J. Virol. **66:**2740–2747.
7. **Bienz, K., D. Egger, M. Troxler, and L. Pasamontes.** 1990. Structural organization of poliovirus RNA replication is mediated by viral proteins of the P2 genomic region. J. Virol. **64:**1156–1163.
8. **Chang, K.-Y., and I. Tinoco.** 1995. Characterization of a "kissing" hairpin complex derived from the human immunodeficiency virus genome. Proc. Natl. Acad. Sci. USA **91:**8705–8709.
9. **Chomczynski, P., and N. Sacchi.** 1987. Single step method of RNA isolation by acid guanidinium thiocyanate-phenol-chloroform extraction. Anal. Biochem. **162:**156–159.
10. **Cui, T., and A. G. Porter.** 1995. Localization of binding site for encephalomyocarditis virus RNA polymerase in the 3′-noncoding region of the viral RNA. Nucleic Acids Res. **23:**377–382.
11. **Frankel, A. D., I. W. Mattaj, and D. C. Rio.** 1991. RNA-protein interactions. Cell **67:**1041–1046.
12. **Harris, K. S., W. Xiang, L. Alexander, W. S. Lane, A. V. Paul, and E. Wimmer.** 1994. Interaction of poliovirus polypeptide $3CD^{pro}$ with the 5′ and 3′ termini of the poliovirus genome. J. Biol. Chem. **269:**27004–27014.
13. **Jacobson, S. J., D. A. M. Konings, and P. Sarnow.** 1993. Biochemical and genetic evidence for a pseudoknot structure at the 3′ terminus of the poliovirus RNA genome and its role in viral amplification. J. Virol. **67:**2961–2971.
14. **Kaine, B. P.** 1990. Structure of the archaebacterial 7S RNA molecule. Mol. Gen. Genet. **221:**315–321.
15. **Klump, W. M., I. Bergmann, B. C. Muller, D. Ameis, and R. Kandolf.** 1990. Complete nucleotide sequence of infectious coxsackievirus B3 cDNA: two initial 5′ uridine residues are regained during plus-strand RNA synthesis. J. Virol. **64:**1573–1583.
16. **Ladner, J. E., A. Jack, J. D. Robertus, R. Brown, D. Rhodes, B. F. C. Clark, and A. Klug.** 1975. Structure of yeast phenylalanine transfer RNA at 2.5 A resolution. Proc. Natl. Acad. Sci. USA **72:**4414–4418.
17. **Laemmli, U. K.** 1970. Cleavage of structural proteins during the assembly of

the head of bacteriophage T4. Nature (London) **227**:680–685.
18. **Lama, J., M. A. Sanz, and P. L. Rodriguez.** 1995. A role of 3AB protein in poliovirus genome replication. J. Biol. Chem. **270**:14430–14438.
19. **Mans, R. M. W., C. W. A. Pleij, and L. Bosch.** 1991. tRNA-like structures. Structure, function and evolutionary significance. Eur. J. Biochem. **201**:303–324.
20. **Marino, J. P., R. S. Gregorian, G. Csankovski, and D. M. Crothers.** 1995. Bent helix formation between RNA hairpins with complementary loops. Science **268**:1448–1454.
21. **Persson, C., E. Gerhart, H. Wagner, and K. Nordström.** 1990. Control of replication of plasmid R1: structures and sequences of the antisense RNA, CopA, required for its binding to the target RNA, CopT. EMBO J. **9**:3767–3775.
22. **Persson, C., E. Gerhart, H. Wagner, and K. Nordström.** 1990. Control of replication of plasmid R1: formation of an initial transient complex is rate-limiting for antisense RNA-target RNA pairing. EMBO J. **9**:3777–3785.
23. **Philippe, C., F. Eyermann, L. Bernard, C. Portier, B. Ehresmann, and C. Ehresmann.** 1993. Ribosomal protein S15 from *Escherichia coli* modulates its own translation by trapping the ribosome on the mRNA initiation loading site. Proc. Natl. Acad. Sci. USA **90**:4394–4398.
24. **Pierangeli, A., M. Bucci, P. Pagnotti, A. M. Degener, and R. P. Bercoff.** 1995. Mutational analysis of the 3′-terminal extra-cistronic region of poliovirus RNA: secondary structure is not the only requirement for minus strand RNA replication. FEBS Lett. **374**:327–332.
25. **Pilipenko, E. V., V. M. Blinov, B. K. Chernov, T. M. Dmitrieva, and V. I. Agol.** 1989. Conservation of the secondary structure elements of the 5′-untranslated region of cardio- and aphtovirus RNAs. Nucleic Acids Res. **17**:5701–5711.
26. **Pilipenko, E. V., A. P. Gmyl, S. V. Maslova, A. P. Belov, A. N. Sinyakov, M. Huang, T. D. K. Brown, and V. I. Agol.** 1994. Starting window, a distinct element in the Cap-dependent internal initiation of translation on picornaviral RNA. J. Mol. Biol. **241**:398–414.
27. **Pilipenko, E. V., S. V. Maslova, A. N. Sinyakov, and V. I. Agol.** 1992. Towards identification of cis-acting elements involved in the replication of enterovirus and rhinovirus RNAs: a proposal for the existence of tRNA-like terminal structures. Nucleic Acids Res. **20**:1739–1745.
28. **Pilipenko, E. V., K. V. Poperechny, S. V. Maslova, W. J. G. Melchers, H. J. Bruins Slot, and V. I. Agol.** Cis-element, oriR, involved in the initiation of (−)strand poliovirus RNA: a quasi-globular multi-domain RNA structure maintained by tertiary ("kissing") interactions. Submitted for publication.
29. **Pleij, C. W. A.** 1990. Pseudoknots: a new motif in the RNA game. Trends Biochem. Sci. **15**:143–147.
30. **Plotch, S. J., and O. Palant.** 1995. Poliovirus protein 3AB forms a complex with and stimulates the activity of the viral RNA polymerase, $3D^{pol}$. J. Virol. **69**:7169–7179.
31. **Reed, L. J., and H. Muench.** 1938. A simple method of estimating fifty percent endpoints. Am. J. Hyg. **27**:493–497.
32. **Rietveld, K., K. Linschooten, C. W. A. Pleij, and L. Bosch.** 1984. The three-dimensional folding of the tRNA-like structure of tobacco mosaic virus RNA. A new building principle applied twice. EMBO J. **3**:2613–2619.
33. **Rietveld, K., R. van Poelgeest, C. W. A. Pleij, J. H. van Boom, and L. Bosch.** 1982. The tRNA-like structure at the 3′ terminus of turnip yellow mosaic virus RNA. Differences and similarities with canonical tRNA. Nucleic Acids Res. **10**:1929–1946.
34. **Rohll, J. B., D. H. Moon, D. J. Evans, and J. W. Almond.** 1995. The 3′ untranslated region of picornavirus RNA: features required for efficient genome replication. J. Virol. **69**:7835–7844.
35. **Rohll, J. B., N. Percy, E. Ley, D. J. Evans, J. W. Almond, and W. S. Barclay.** 1994. The 5′ untranslated regions of picornavirus RNAs contain independent functional domains essential for RNA replication and translation. J. Virol. **68**:4384–4391.
36. **Sarnow, P., H. D. Bernstein, and D. Baltimore.** 1986. A poliovirus temperature-sensitive RNA synthesis mutant located in a noncoding region of the genome. Proc. Natl. Acad. Sci. USA **83**:571–575.
37. **Schmidt, N. J.** 1979. Cell culture techniques for diagnostic virology, p. 65–139. *In* E. H. Lennette, and N. J. Schmidt (ed.), Diagnostic procedures for viral, rickettsial and chlamydial infections. American Public Health Association, Washington, D.C.
38. **Struck, J. C. R., and V. A. Erdmann.** 1990. Phylogenetic and biochemical evidence for a secondary structure model of a small cytoplasmic RNA from *Bacilli*. Eur. J. Biochem. **192**:17–24.
39. **Sugimoto, N., R. Kierzek, S. M. Freier, and D. H. Turner.** 1986. Energetics of internal GU mismatches in ribo-oligonucleotide helixes. Biochemistry **25**:5755–5759.
40. **Sussman, J. L., and S.-H. Kim.** 1976. Three-dimensional structure of a transfer RNA in two crystal forms. Analysis of three sets of atomic coordinates of yeast phenylalanine tRNA establishes common features. Science **192**:853–858.
41. **Takeda, N., R. J. Kuhn, C.-F. Yang, T. Takegami, and E. Wimmer.** 1986. Initiation of poliovirus plus-strand RNA synthesis in a membrane complex of infected HeLa cells. J. Virol. **60**:43–53.
42. **Tang, C. K., and D. E. Draper.** 1989. Unusual mRNA pseudoknot structure is recognized by a protein translation repressor. Cell **59**:511–536.
43. **Todd, S., J. H. C. Nguyen, and B. L. Semler.** 1995. RNA-protein interactions directed by the 3′ end of human rhinovirus genomic RNA. J. Virol. **69**:3605–3614.
44. **Toyoda, H., C. F. Yang, N. Takeda, A. Nomoto, and E. Wimmer.** 1987. Analysis of RNA synthesis of type 1 poliovirus by using an in vitro molecular genetic approach. J. Virol. **61**:2816–2822.
45. **van Kuppeveld, F. J. M., J. M. D. Galama, J. Zoll, and W. J. G. Melchers.** 1995. Genetic analysis of a hydrophobic domain of coxsackie B3 virus protein 2B: a moderate degree of hydrophobicity is required for a *cis*-acting function in viral RNA synthesis. J. Virol. **69**:7782–7790.
46. **Weiner, S. J., P. A. Kollman, D. T. Nguyen, and D. A. Case.** 1986. An all atom force field for simulations of proteins and nucleic acids. J. Comp. Chem. **7**:230–252.
47. **Wimmer, E., C. U. T. Hellen, and X. Cao.** 1993. Genetics of poliovirus. Annu. Rev. Genet. **27**:353–436.
48. **Zoll, J., P. Jongen, J. Galama, F. van Kuppeveld, and W. Melchers.** 1993. Coxsackievirus B1-induced murine myositis: no evidence for viral persistence. J. Gen. Virol. **74**:2071–2076.
49. **Zoll, J., J. Galama, and W. Melchers.** 1994. Intratypic genome variability of the coxsackievirus B1 2A protease region. J. Gen. Virol. **75**:687–692.
50. **Zwieb, C.** 1989. Structure and function of signal recognition particle RNA. Prog. Nucleic Acid Res. Mol. Biol. **37**:207–234.